Electronical Supporting Information

Trapping of Sub-100 nm Nanoparticles Using Gigahertz Acoustofluidic Tweezers for Biosensing Applications

Weiwei Cui [a,b)#], Luye Mu [b)], Xuexin Duan [a)*], Wei Pang [a)], and Mark A. Reed [a,b)*]

[a)] State Key Laboratory of Precision Measuring Technology & Instruments, College of Precision Instrument and Optoelectronics Engineering, Tianjin University, Tianjin 300072, China.

[b)] Department of Electrical Engineering and Yale University, New Haven, Connecticut 06520, United States

Table of contents

1. Simulation details.

First of all, we studied the resonating mode of the resonator in air, with the aim to quantitatively characterize the acoustic fields. A three-dimensional finite-element analysis model was built with COMSOL 5.0, of which the geometric structure and meshed structures are prospectively presented in Figure. S1a-b. The vibration of the resonator is governed by equations[1]:

$$c^E\frac{\partial^2 u}{\partial x^2} + e\frac{\partial^2 \varphi}{\partial x^2} = -\rho\omega^2 u \quad (1)$$

$$e\frac{\partial^2 u}{\partial x^2} - \varepsilon^S\frac{\partial^2 \varphi}{\partial x^2} = 0 \quad (2)$$

Where, u and φ are respectively the mechanical displacement and electrical potential; ρ, c^E, ε^S, e are the properties of the piezoelectric material, and they respectively are: density, stiffness, dielectric constant, and piezoelectric constant.

Actually, by combing equation (1), (2) with Newton's second law (F=ma), the wave equation can be obtained.

$$\frac{\partial^2 u}{\partial t^2} = \frac{c\partial^2 u}{\rho\partial z^2} \quad (3)$$

The parameters of piezoelectric layer and metal electrodes are given by the COMSOL models, which can be directly used. And the thickness of the TE, PZ, and BE are respectively 100, 1500, and 100 nm. The 3D simulated vibration field of the resonator is presented in Figure. 2c.

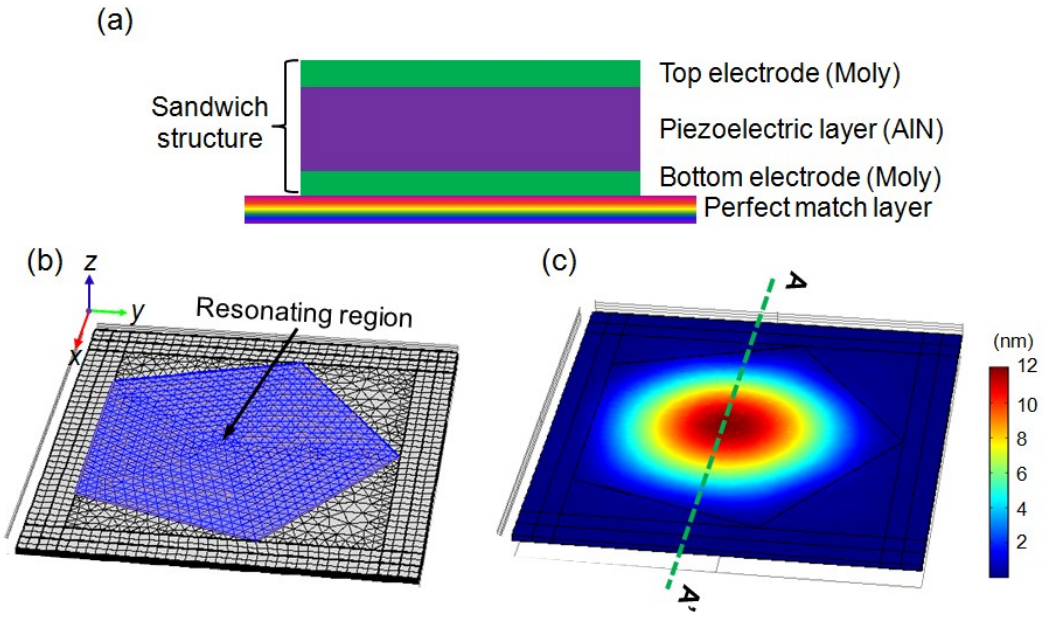

Figure. S1 (a) Schematic of the simplified resonator model (cross-section) in COMSOL simulation, with Bragg reflector considered as a perfect match layer. (b) Meshed result of the 3D resonator. (c) Simulated vibrating field (confined in the pentagon region) at resonating frequency. The structure in (a) is from the cross-section view of A-A' in (c).

Because the physics on the interface between GHz vibration substrate and the liquids have not been well understood so far, we choose to build up a pure fluidic model with the calculated forces induced by the resonator as the boundary conditions, instead of constructing a united model that directly couples GHz vibration with liquids. Therefore, we firstly consider physical situation of GHz acoustic fields in liquid environment. When acoustic waves travel from solid to liquid, acoustic decay would occur in the solid-liquid interface due to the mismatch of acoustic impedance between two different mediums. For longitudinal acoustic wave generated by our resonator, the attenuation coefficient (β) is expressed as[2, 3]

$$\beta = \frac{b\omega^2}{\rho_l {c_l}^3} \quad (4)$$

with $$b = \frac{4}{3\mu + \mu'} \quad (5)$$

Here, ρ_l, c_l are respectively density and sound speed in the liquid, and μ, μ' are respectively dynamic and bulk viscosity of the liquid.

Equation (4) reveals that the decay length (β^{-1}) scales with ω^{-2}. Thus, gigahertz acoustic waves would decay rapidly in the liquid, generally within several wavelengths (in the order of ~1 μm). Such a short decay length contributes to couple most of the acoustic energy into the microfluidics, as well as avoids the formation of standing waves

in the microchannel, which is significant for the generation of strong micro-streaming. The body force (F_B, in N/m^3) produced at a point (x, z) in the fluid is expressed as

$$F_B = \rho\beta v(x,z)^2 \quad (6)$$

Where, $v(x,z)$ is the vibration displacement velocity of the resonator surface, which can be calculated from the simulated result in Figure. S1c.

The GHz acoustic wave would provide much stronger body forces to launch the fluid away from the resonator surface. Generally, the actuated fluids move towards the microchannel boundaries (or top plate) and then be reflected by them, resulting in micro-vortices at the edges of the acoustic fields. As localized acoustic fields trigger body force within a rather short decay length, large pressure gradients would be formed in the horizontal and vertical directions, which contribute to generate micro-vortices within the microfluidic systems.

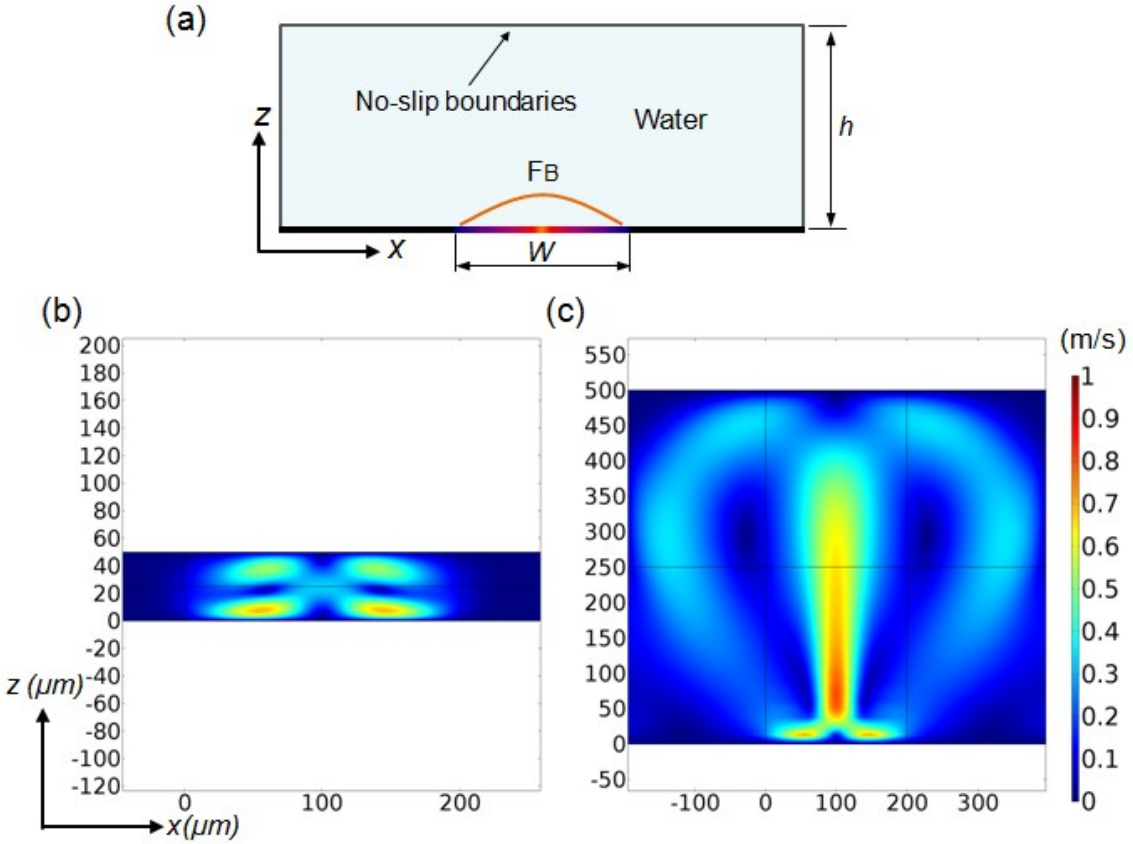

Figure. S2 (a) Boundary conditions of the acoustofluidic simulation with a pure fluidic model; Simulated velocity field with fluidic height of (b) 50 μm and (c) 500 μm.

To evaluate the microfluidic stream triggered by GHz acoustic waves, a finite element simulation of the fluid motion in a spatial confined of 105 μm height has been carried out. Figure.S2a presents the boundary conditions of the acoustofluidic

chip. The acoustic streaming response of the fluid was characterized by the second-order system of equations, which in turn is driven by the first-order equations. The fluid response is governed by the standard Navier–Stokes equation for a linear, viscous compressible fluid. In our case, GHz acoustic waves induced body force on the resonator-liquid interface was introduced into the Navier-Stokes equation by presetting a boundary condition.[3]

$$\rho\vec{V}\cdot\nabla\vec{V}+\nabla\cdot P-\mu\nabla^2\vec{V}=\vec{F}_B \qquad (7)$$

where $\vec{V}$ is the velocity vector, P is the pressure, and ρ, μ denote the density and viscosity of the fluid, respectively.

Due to the fact that the acoustic decay rapidly into the liquid, as well the focused distribution of acoustic fields on the substrate (Figure. 1c), the distribution of body force should be considered for a reasonable calculation. Combing data acquired from the acoustic vibration fields with the acoustic decay theory, expressions if the body force in the x-direction and z-direction can be written as

$$F_x=\frac{2k^2}{\alpha}u_0{}^2\sin(2\alpha x)e^{-2\beta z} \qquad (8)$$

$$F_z=2\beta u_0{}^2e^{-2\beta z} \qquad (9)$$

Where, k, u_0 are respectively the acoustic wave number and applied voltage. $\alpha=\frac{\pi}{W}$, wherein w is the width of the resonator.

We use Nyborg's perturbation approach[4] where the fluid velocity, pressure and density are assumed to be of the following form

$$\begin{aligned}V&=V_0+\varepsilon V_1+\varepsilon^2V_2+O(\varepsilon^3)+\ldots\\P&=P_0+\varepsilon P_1+\varepsilon^2P_2+O(\varepsilon^3)+\ldots\\\rho&=\rho_0+\varepsilon\rho_1+\varepsilon^2\rho_2+O(\varepsilon^3)+\ldots\end{aligned} \qquad (10)$$

where ε is a non-dimensional parameter defined as the ratio of the in-situ body force to that in the resonator centre. Substitution of Eq. (10) in Eq. (7), and segregation of first-order term yields a first-order system.

$$\rho\vec{V}_1\cdot\nabla\vec{V}_1+\nabla\cdot P_1-\mu\nabla^2\vec{V}_1=\vec{F}_B \qquad (11)$$

Following the same procedure for the second-order term, we can also obtain the second-order system. Finally, the first and second-order system equations are successfully solved to obtain the stream velocity field of the fluidic (Figure S2b, c).

Parameters used in the COMSOL simulation.

Parameter	Value
Water density	1000 kg/m^3
Water bulk viscosity	1.0087×10^{-3} Pa•s
Water dynamic viscosity	1.0100×10^{-3} Pa•s
Acoustic speed in water	1488 m/s
Acoustic frequency	1970 MHz
Acoustic vibrating magnitude	10 nm
Acoustic wavelength	1 μm
Resonator width	200 μm

2. Calculation of signal enhancement

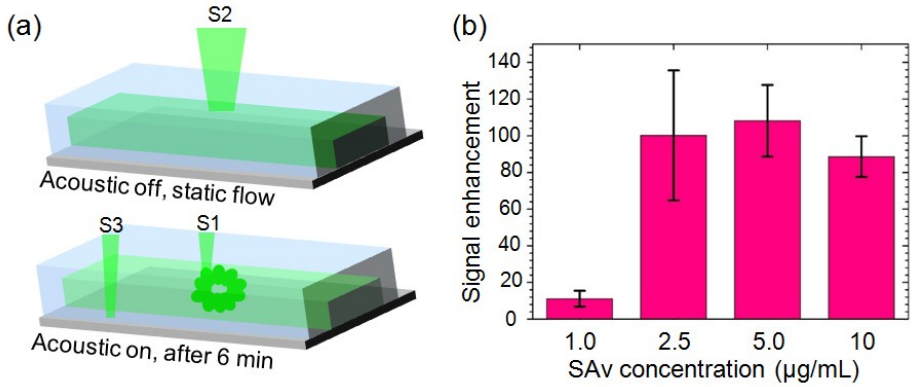

Figure. S3 Signal enhancement of different SAv concentrations. As labeled in the insert in (a), fluorescence intensity (FI) in regions S1 (enriched value), S3 outside the channel (background value), and S2 that only FITC-SAv is filled in the channel (reference values, not labelled in the figure are acquired to calculate the signal enhancement (*EH*) by equation *EH=(S1-S3)/(S2-S3)*. (b) The signal enhancement of SAv detection in serum.

3. Portable operating strategies.

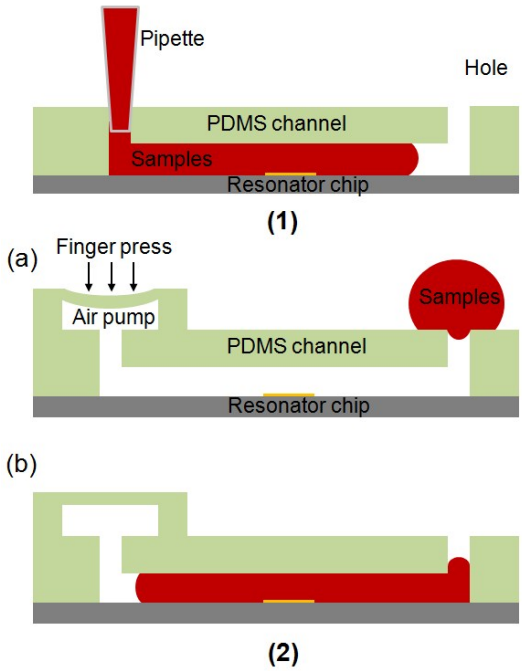

Figure S4. Schematic of two portable AFT examples: (1) samples loading with a pipette; (2) integrating a finger-pressing pump with the AFT that can be operated easily by: (a) pressing the air chamber and then loading the samples on the input hole; (b) releasing the press to "drink" the samples into the channel via air pressure. Red color presents detected samples.

Another example of a simple, offline bioassay that does not require any microfluidics is shown in Figure. S5. Droplets can be generated and dispensed onto the AFT via pipette loading, inject-printing, or electro-wetting. To confine the droplet to the AFT region, a surrounding hydrophobic surface (Figure. S5a) easily confines the droplets. Figure. S5b shows a simulated velocity field for such a drop, illustrating that even for a macroscopic droplet a trapping vortex is created. We do note that compared with the vortex in a microchannel, the velocity for a droplet is reduced and the concentration volume is increased; nonetheless, it is sufficient for trapping. Figure. S5c shows a vortex formation of beads in a millimeter-sized drop. The advantage of this variant of the AFT is portability, and the ability to image by eye of with a cellphone camera, enabling POC or in-field applications.

According to discussions in Figure. 2, for maximum trap efficiency, the size of the droplet is determined by the AFT device size. There is an optimal drop size for generating strongest vortex in the AFT, with a fluid height to device width ratio (*h*/*w*) of ~1. Simulations from varying the device width shows that the maximum velocities are always achieved when *h*~*w*. Thus, the optimal device size will depend on the chosen sample volume; i.e., a picolitre drop would require a device size ~10 µm.

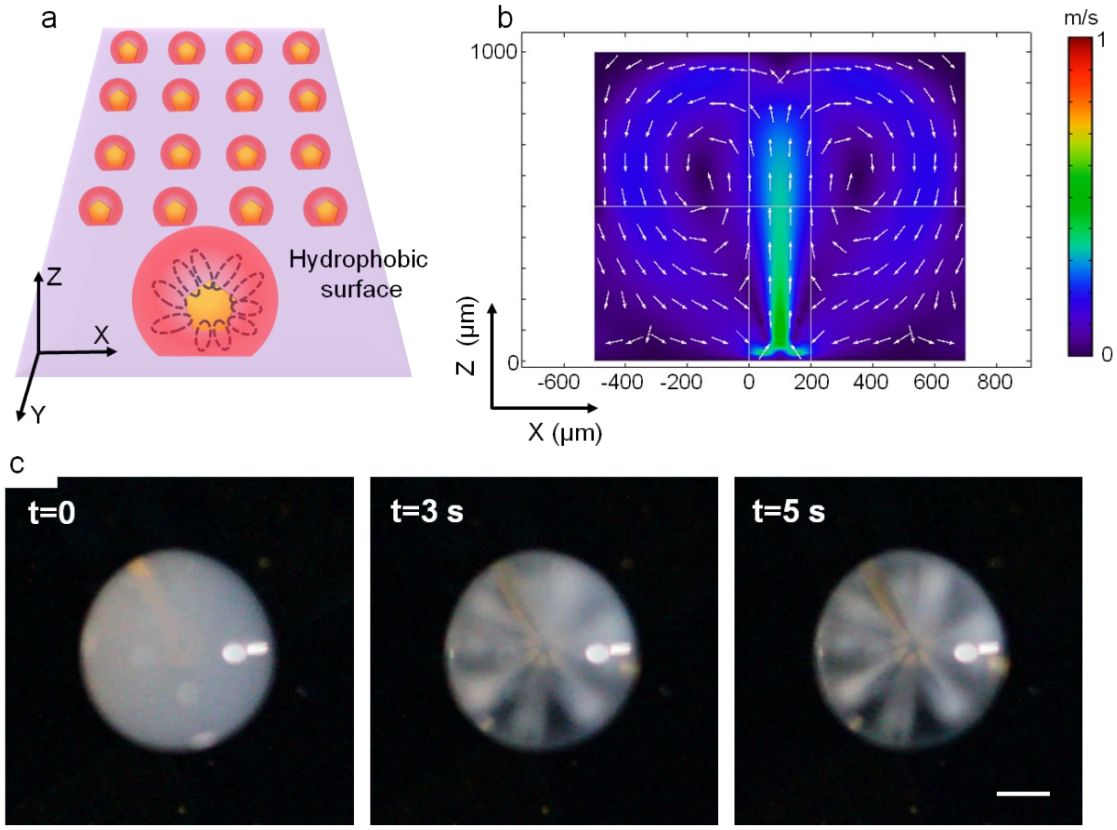

Figure S5. Droplet bioassay for portable detection. (a) Schematic of droplet-AFT biosensing platform. (b) Simulated velocity field of the vortex within a millimeter liquid to present the streaming phenomenon inside the droplets. (c) Nanoparticle (polystyrene particle with a diameter of 300 nm) trapping and enriching inside a 2 µL droplet. The applied power is 50 mW. Scale bar in (c) is 200 µm.

4. Fabrication of AFT chip.

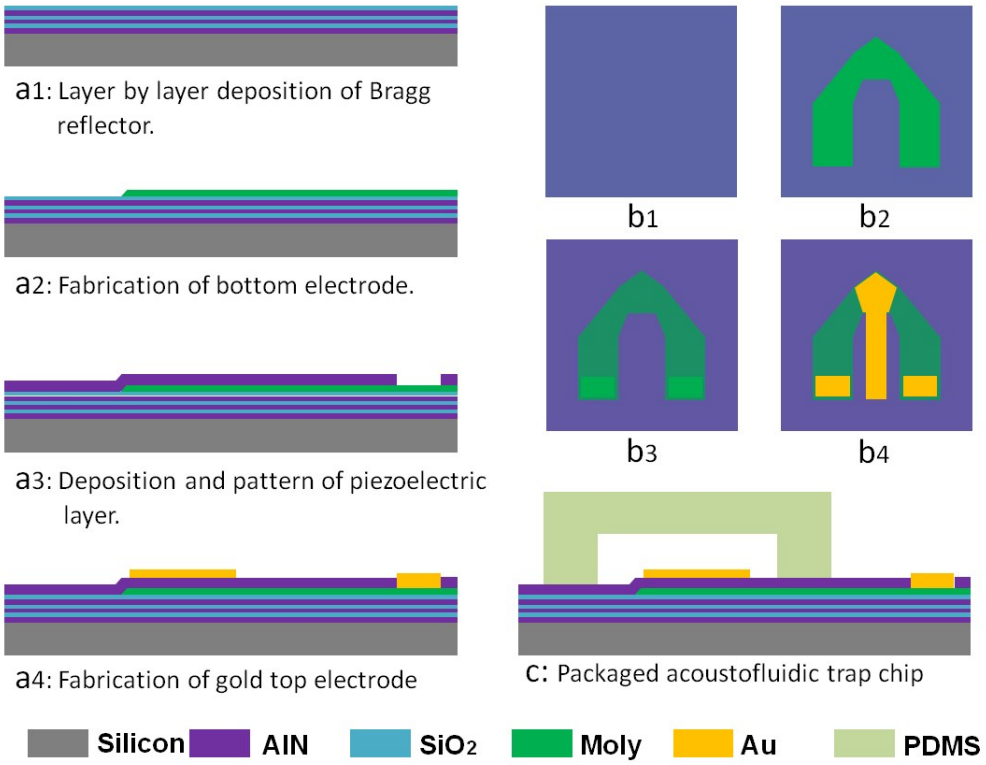

Figure. S6 Fabrication process of the acoustofluidic trap: (a) cross-section view of the stacks of the device; (b) top view of the device layout, with bi corresponding to ai (i=1,2,3,4); (c) cross-section view of packaged acoustofluidic chip. Abbreviation: AlN, Aluminum Nitride; $Si0_2$, Silicon Oxide; Moly, Molybdenum, Au, Aurum; PDMS, PolyDiMethylSiloxane.

References:

1. Auld, B. A. *Acoustic fields and waves in solids*. Рипол Классик: 1973.
2. Frommelt, T.; Kostur, M.; Wenzel-Schäfer, M.; Talkner, P.; Hänggi, P.; Wixforth, A. Microfluidic mixing via acoustically driven chaotic advection. *Physical review letters* 2008, 100, 034502.
3. Cui, W.; Zhang, H.; Zhang, H.; Yang, Y.; He, M.; Qu, H.; Pang, W.; Zhang, D.; Duan, X. Localized ultrahigh frequency acoustic fields induced micro-vortices for submilliseconds microfluidic mixing. *Applied Physics Letters* 2016, 109, 253503.
4. Longuet-Higgins, M. S. In *Viscous streaming from an oscillating spherical bubble*, Proceedings of the Royal Society of London A: Mathematical, Physical and Engineering Sciences, The Royal Society: 1998; pp 725-742.